

# Metallicity determination in gas-rich galaxies with semiempirical methods.

A.M. Hidalgo-Gómez

*Department of Physics, Escuela Superior de Física y Matemáticas, IPN, U.P. Adolfo López Mateos, C.P. 07738, Mexico city, Mexico*

and D. Ramírez-Fuentes

*Instituto de Astronomía, UNAM, Ciudad Universitaria, Apto. 70 264, C.P. 04510, Mexico City, Mexico*

## ABSTRACT

A study of the precision of the semiempirical methods used in the determination of the chemical abundances in gas-rich galaxies is carried out. In order to do this the oxygen abundances of a total of 438 galaxies were determined using the electronic temperature, the  $R_{23}$  and the P methods. The new calibration of the P method gives the smaller dispersion for the low and high metallicity regions, while the best numbers in the turnaround region are given by the  $R_{23}$  method. We also found that the dispersion correlates with the metallicity. Finally, it can be said that all the semiempirical methods studied here are quite insensitive to metallicity with a value of  $8.0 \pm 0.2$  dex for more than 50% of the total sample.

## 1. Introduction

The determination of nebular abundances in H II regions is not a simple matter. It is well known that the ionic abundances depend on the intensity of the lines involved, and on the electronic density and temperature (Peimbert & Torres-Peimbert 1977; Aller 1984; Osterbrock 1989). For nearby bright galaxies, the weak auroral lines needed for the electronic temperature ( $T_e$ ) determination can be detected when the signal-to-noise (S/N) is high enough. When the  $T_e$  is determined, the ionic abundances can be easily obtained through the emissivities of the specific ions, when a certain ionization structure for the nebulae is assumed (e.g., Aller 1984; Izotov et al. 2006 for a more recent review). Such a procedure is normally called the “standard method” for the abundance determination. The most important caveat concerning the standard method is that the auroral lines are always very weak. The typical uncertainty associated with the standard method is about 0.1 dex (Kewley & Ellison 2008) but this increase significantly for low S/N spectra.

The situation gets worse when the forbidden auroral lines are absent. The most common reason for such absence is the low S/N of the spectra but it is not the only one (see Hoyos & Díaz 2006). In such situations the so-called semiempirical, or bright-line, methods need to be used in order to

determine the metal content of the H II region. The most common and popular of these methods is the  $R_{23}$  calibrator proposed by Pagel et al. (1979) and improved by McGaugh (1991), among others. Other calibrations of the  $R_{23}$  method have been proposed using larger samples and more complete stellar evolutionary grids (e.g. Zaritsky et al. 1994; Kewley & Dopita (2002); Kobulnicky & Kewley 2004). We prefer to use the calibration by McGaugh (1991). The main reason is that, although this calibration is old, it takes into account the influence of the ionization parameter on the chemical abundance determination.

In recent years, many other semiempirical methods have been proposed, based on the same lines as the  $P$  method (Pilyugin 2000,2001; Pilyugin & Thuan 2005), or on the nitrogen (the  $N2$ , Denicoló et al. 2002) or the sulfur lines (the  $S_{23}$ , Díaz & Pérez-Montero 2000; the  $S_{234}$ , Oey & Shields 2000)

All of the semiempirical methods present problems: bivaluation, large dispersion, dependence on other parameters (such as the ionization parameter or the nitrogen abundance), very large wavelength range between the lines involved, etc. Moreover, the large dispersion in the metallicity values obtained with the semiempirical methods can be due to the different H II regions geometries (which amount to different ionization parameters) and differences in age of the H II regions used for the calibration of the semiempirical methods. In addition, there are other influences such as the different apertures for different spectra which might mask the real calibration of the semiempirical methods (A.M. Hidalgo-Gómez 2009, in preparation).

The main interest of this investigation is to determine whether any of the semiempirical methods available or any of their different calibrations give better oxygen abundances than the others. In order to make such a comparison we think that the standard method abundances are good touchstones. The idea for this investigation comes out from the necessity of reliable abundance determinations with any of the semiempirical methods for a sample of dwarf spiral galaxies where the [OIII]  $\lambda 4363$  is not detected (A.M. Hidalgo-Gómez et al 2009, in preparation). It is well known that galaxies with and without the [OIII] $\lambda 4363\text{\AA}$  line have different properties on the  $T_e$  range, ionization parameter, and luminosity (Hoyos & Díaz 2006). Therefore, the metal contents might significantly differ. Although we are aware of this, studies such as the one presented here might give some clues about the goodness of each of the semiempirical methods.

In the next section, the description of the sample of galaxies used in this investigation is carried out, while the comparison of the standard method with the semiempirical methods used is presented in Section 3. A comparison with other studies already published is presented in Section 4, and a brief discussion is given in Section 5. Finally, conclusions are presented in Section 6.

## 2. Description of the data and the methods

A homogeneous sample is needed in order to make a proper study of the difference in the chemical abundances provided by different methods. By homogeneous we mean a sample observed,

reduced, and analyzed in the same way in order to reduce the dispersion of the results. Moreover, in order to consider the effects of the age of the H II regions, the galaxies should be of similar morphological type. However, most of the studies done so far on the calibrations of the semiempirical methods use samples of galaxies where the oxygen abundances have been collected from the literature. Such a procedure might not be very appropriated, leading to results that are not very reliable.

In order to take into account all of the possible sources of dispersion, we used a sample as homogeneous as possible and also large enough to achieve conclusive results. The sample consists of a total of 438 galaxies from Kniazev et al. (2004), mainly blue compact (392) and irregular galaxies (28). They were selected from a sample of 612 galaxies observed by Sloan Digital Sky Survey (SDSS) where the oxygen line [O III]  $\lambda 4363$  is detected. Therefore, the electronic temperature can be determined and the standard method can be used for the determination of the chemical abundances for all the galaxies. We chose only those galaxies with [O II]  $\lambda 3727$  detected in order to decrease the uncertainties.

The main caveat of this sample is that, any sample selected by the presence (or absence) of a particular spectral line is biased in itself. This should be taken into account when applying any calibration based on a sample of galaxies with the [O III]  $\lambda 4363\text{\AA}$  line to objects where this line is absent or to a sample with different systematics than those presented here. In particular, those galaxies with the presence of the [O III]  $\lambda 4363\text{\AA}$  line seem to show higher ionization parameters and less evolved stellar population than those galaxies without it (Hoyos & Díaz 2006). In addition, the equivalent width (EW) of H $\beta$  is much larger (a factor of 2.8) for the galaxies in the first group than those galaxies without the [O III]  $\lambda 4363\text{\AA}$  line.

One of the most interesting parameters in the characterization of the H II regions is the ionization parameter. It depends on the ionizing continuum and on the geometry of the region. The ionization parameter is defined in terms of a uniform density,  $n_e$ , by  $U = L/4 \pi R_s^2 c$ , where  $R_s^2$  is the Strömberg radius and  $L$  is the H-ionizing photon luminosity (Mathis 2000). As we will discuss later, some of the semiempirical methods depend on this parameter. Therefore, it will be very interesting to study the distribution of the ionization parameter in our sample of galaxies. A simple way of doing this is through the ratio [O II]/[O III]. More than half of the galaxies in our sample have values of this ratio between 0.5 and 1: only 6% show ratios larger than 1.2 and only 3% smaller than 0.1. These values are slightly smaller than those of the [O III]  $\lambda 4363$  galaxies in Hoyos & Díaz (2006). One reason for these differences might be that here we have considered only one of the [O III] lines (at  $5007\text{\AA}$ ). We can also check if the  $T_e$  (and, therefore, the abundances) depends on the ionization parameter. Such a relationship is clear for a small sample of H II regions in nearby dwarf irregular galaxies (A.M. Hidalgo-Gómez, unpublished results). It is apparent from Figure 1 that there is no correlation between  $T_e$  and the  $\log([O II]/[O III])$  for those galaxies with temperatures smaller than 14,000 K and therefore, between the oxygen content and the ionization parameter. However, for those galaxies with  $T_e$  higher than 14,000 K, there is a group of galaxies with a negative trend (very low values of  $\log([O II]/[O III])$ ) and another with a positive one

( $\log([\text{O II}]/[\text{O III}]) \approx 0.5$ ). In any case, the number of those galaxies is very small (less than 10%) to have a great influence on our results.

### 2.1. On the standard method

The standard method (SM) abundance were determined by us from the extinction (and absorption) corrected line intensities given by Kniazev et al. (2004) with a five-level atom two-zone model (N. Bergvall 1999, private communication). A density of  $100 \text{ cm}^{-3}$  was considered for all the spectra. The electronic temperature of the  $\text{O}^{++}$  is determined with the ratio between the nebular and the auroral oxygen lines, while the temperature of the  $\text{O}^+$  zone is based on photoionization models. From these values a parametrization can be obtained as

$$T(\text{O}^+) = 6520 + 0.50T(\text{O}^{++}). \quad (1)$$

The average uncertainty of this equation is about 300 K.

In order to see if the parametrization gives the correct values for the  $T(\text{O}^{++})$  a comparison with other procedures can be done.

The electronic temperature of the  $\text{O}^+$  can be determined from the ratio of the intensities of the  $[\text{O II}]$  lines at  $\lambda, 3726, 3739$  and  $\lambda, 7319, 7320$ . We found two different equations that related the  $T(\text{O}^+)$  and this ratio (hereafter, RO2).

$$T(\text{O}^+) = 0.853/\log(I_{3727}/I_{7325}) - 0.928 + \log(1 + 7.03 x) + 0.02 \log t \quad (2)$$

where  $I_{3727}$  is the intensities of the lines  $[\text{O II}]\lambda, 3726, 3729$ ,  $I_{7325}$  the intensities of the lines  $[\text{O II}]\lambda, 7320, 7330$ ,  $t$  is the  $T(\text{O}^{++})$  in units of  $10^4$ , and  $x = 0.01N_e/T_e$  where  $N_e$  is the electronic density (Hägele et al. 2008). The other equation is

$$T(\text{O}^+) = a_o + a_1 \text{RO2} + a_2/\text{RO2} \quad (3)$$

with  $a_o = 0.23 - 0.0005 n - 0.17/n$ ,  $a_1 = 0.0017 + 9 \cdot 10^{-6} n + 0.0064/n$ , and  $a_2 = 38.3 - 0.021 n - 16.4/n$ , where  $n$  is the density (Hägele et al. 2008).

When the auroral lines cannot be detected because of the low S/N or the small wavelength range of the spectra, the  $T(\text{O}^+)$  can be determined from the parametrization between  $T(\text{O}^+)$  and  $T(\text{O}^{++})$  using photoionization models, such as, e.g., Campbel et al. (1986), or using observational data such as Pilyugin et al. (2006). In order to see how accurate our equation is, we have compared the  $T(\text{O}^+)$  determined from it with the values obtained with the parametrizations by Pagel et al. (1992), Izotov et al. (2006), Deharveng et al. (2000), Pilyugin et al. (2006), Pérez-Montero & Díaz (2003), Campbell et al. (1986), Garnett (1992), and Oey & Shields (2000). The latter three

are identical and are based on Stasińska’s (1980) models. For all of parametrizations studied, the average differences are less than 500 K, except for that of Pilyugin et al. (2006), for which the average difference is of the order of 800 K. Therefore, our  $T(O^+)$  value agrees with those obtained from other parametrizations. We also determined the  $T(O^+)$  from the RO2 ratio using the intensities of  $\lambda 7320 + \lambda 7330$  given by Kniazev et al. (2004). The determination was done using both Equations (2) and (3). In both cases, the differences between the  $T(O^+)$  from equation 1 (or from any of the parametrizations detailed above) and from equations 2 and 3 are about 3000 K. We think that this is due to more deeper problems which are out of the scope of this paper and which might be studied in detail in a separate paper. In any case, the values of the  $T(O^+)$  used here in the oxygen abundance determinations are not worse than any other determined from parametrizations.

The uncertainties in the oxygen abundances determined here were obtained from the uncertainties in the line intensities reported by Kniazev et al. (2004). The error bar was made symmetric with the mean value taken as the nominal value. The average uncertainty in the oxygen abundance is about 0.08 ( $\sigma = 0.03$ ). Only 9% of the uncertainty values are larger than  $2\sigma$ . The differences between the uncertainties determined by us and those reported by Kniazev et al. (2004) in their table 4 are less than 0.02 for the majority of the galaxies.

The next thing to be done before comparing the standard method with the semiempirical methods is to test the internal consistency of the standard method itself. It is important to know how accurate the values obtained by our code are compared with other values obtained from other procedures. It is claimed that differences in the procedures might result in important differences in the  $T_e$  and, therefore, in the oxygen abundances.

In order to check this, we compared our abundance data with those obtained from the formalism of (1) Kniazev et al. (2004), (2) Izotov et al. (2006), and (3) Aller (1984). The results are shown in Table 1. The first row shows the average differences in the oxygen abundances between our values and those listed above. The second row shows the percentages of those values which have differences larger than the average uncertainties. The percentages of those values with no differences at all are shown in the third row. It can be seen that the largest differences are obtained with the expression by Izotov et al. (2006), while the other two oxygen abundances are almost identical to our values. This is in good agreement with Izotov et al. (2006), who claimed that the differences in the oxygen abundances are only 1% when the original equations by Aller (1984) are used in their derivation.

## 2.2. On the semiempirical methods

As previously said, there are several methods based on the calibration of the strongest spectral lines to derive chemical abundances, usually oxygen abundances, when the auroral transitions are not detectable. The most common are those based on the  $[OII]+[OIII]/H\beta$  ratio, in particular, the  $R_{23}$  calibrator proposed by Pagel et al. (1979) and the  $P$  method. There are some other

methods for determining the chemical abundances based on other lines: the  $S_{23}$  (Díaz & Pérez-Montero 2000),  $S_{234}$  (Oey & Shields 2000), the  $[N\text{ II}]/H\alpha$  ratio (Denicoló et al. 2002), the  $S_{23}/O_{23}$  parameter (Pérez-Montero & Díaz 2005, and the O3N2 by Pettini & Pagel (2004). We did not study them because the lines needed are not available for the sample we used.

The  $R_{23}$  method is based on the behaviour between the  $[O\text{ II}]+[O\text{ III}]/H\beta$  ratio (the  $R_{23}$ ) and the metallicity. The former increases while diminishing the latter because of both the enhanced heating and the diminished cooling (mainly due to  $O^{++}$ ,  $O^+$ , and  $S^{++}$ ). Therefore, at low metallicity the  $R_{23}$  ratio increases with the oxygen abundances. At high metallicities, the greater cooling efficiency pushed more of the collisionally excited lines energy into the infrared, and  $[O\text{ II}]+[O\text{ III}]/H\beta$  increases with diminishing oxygen abundance. The validity of this method depends on the existence of a statistical relationship between the ionization temperature of the hottest stars ( $T_{ion}$ ) and the oxygen abundances (Pagel et al. 1979). Therefore,  $[O\text{ II}]+[O\text{ III}]/H\beta$  is nearly invariant with respect to the geometrical factors (not with the ionization factor) but varies smoothly with the  $T_{ion}$  (Olofsson 1997).

In his study, McGaugh (1991) used the photoionization code CLOUDY to reproduce detailed H II regions models. He used star clusters as ionizing source of the H II regions, and the metallicity of the ionizing stars is taken into account. The main caveat is that the clusters are zero-age and any evolutionary effect influencing the equivalent effective temperature is taken into account. Also, he considered the dependence on the ionization parameter of the ratio  $[O\text{ II}]+[O\text{ III}]/H\beta$ . He found that such dependence varies with the metallicity so that the parametrization is not easy. In any case, a set of equations can be obtained for each of the branches in which the metallicity range is divided. The main caveat is that photoionization models have serious problems of uniqueness of fitting because there are many disposable parameters: the  $T_{ion}$  of the star(s), the chemical composition, the clumpiness of the density, the geometrical factors, etc, (Pagel et al. 1979). All of them affect the size of the H II regions and, therefore, the state of ionization. Considering all the problems, the estimated accuracy of this calibration is about 0.15 dex (Kewley & Ellison 2008). Hereafter, the abundance determined with this calibrator will be called the  $R_{23}$  abundance.

The next method we studied is the one introduced by Pilyugin (2000, 2001). He introduced a new parameter (the  $P$  parameter) defined as the contribution of the radiation on the lines  $[O\text{ III}]\lambda, \lambda 4959, 5007$  and  $[O\text{ II}]\lambda, \lambda 3726, 3729$  to the total oxygen radiation and calibrated it for a sample of H II regions. Such a parameter corrects for the effect of the ionization parameter and takes into account the physical conditions of the regions because it is an indicator of the hardness of the ionizing radiation. Recently, a new sample was used to recalibrated the high-metallicity region (Pilyugin & Thuan 2005). They used a large sample of data which includes the entire range of excitation. Hereafter, the abundance determined with this method will be called the  $P$  abundance.

### 3. Standard versus semiempirical methods

In order to know which method yields abundance determination closer to those derived by the SM, the abundances determined with the SM and with each one of the semiempirical methods for all the galaxies in the sample were compared. As previously said, our sample has been observed, reduced, and analyzed in the same way. Therefore, the differences in the abundances between the different methods cannot be due to differences in the analysis.

In the calibration of the  $R_{23}$  parameter three branches are differentiated: the low-metallicity branch ( $12+\log(\text{O}/\text{H}) < 8.1$ ), the high-metallicity branch ( $12+\log(\text{O}/\text{H}) > 8.4$ ), and the “turnaround” region ( $8.1 < 12+\log(\text{O}/\text{H}) < 8.4$ ; e.g., McGaugh 1991). Pilyugin (2000) obtained a good correlation between his  $P$  parameter and the oxygen abundances for  $12+\log(\text{O}/\text{H}) < 7.95$  and  $12+\log(\text{O}/\text{H}) > 8.2$ . Afterwards, he divided his sample into two regions: the low metallicity ( $12+\log(\text{O}/\text{H}) < 8.2$ ) and the high metallicity one ( $12+\log(\text{O}/\text{H}) > 8.2$ ; Pilyugin 2001). Combining these two partitions and the results of figure 2, we decided to divide the total sample into three different regions: the low-metallicity ( $12+\log(\text{O}/\text{H}) < 7.95$ ), the high-metallicity branch ( $12+\log(\text{O}/\text{H}) > 8.2$ ), and the “turnaround” region ( $7.95 < 12+\log(\text{O}/\text{H}) < 8.2$ ) in order to simplify the study. We have also taken into account the necessity of a detailed study of the “turnaround” region, which seems to be the most troublesome; e.g., Melbourne & Salzer (2002) did not use the  $R_{23}$  abundances for those galaxies of their sample located at this region due to their low confidences on the results. In order to do such study, a sufficient width in the “turnaround” region is needed, which will not be reachable if the traditional cut at 8.1 and the cut of the high-metallicity region by Pilyugin at 8.2 is considered. Instead, we used the first cut of the low-metallicity region by Pilyugin (2000) at 7.95 as the lower limit of the “turnaround” region. The main caveat might be that our regions are very small. Our “turnaround” region is only 0.05 dex smaller than the one defined by McGaugh (1991). Our high metallicity region ends up at 8.5, mainly due to the requirement that the galaxies in the sample should have the oxygen auroral transition line detected. This line is not easily detected for metallicities above 8.5. The problem in the low-metallicity region is due to the original sample itself. The number of low-metallicity galaxies detected by SDSS is very small: only 200 in front of several thousands of galaxies with metallicities larger than 7.5 were obtained in the later release (Thuan 2008). Therefore, the number of very low-metallicity galaxies in the first releases of SDSS is very small.

With such limits, we can say that in our sample there is a total of 65 galaxies in the high-metallicity region, 100 in the low-metallicity one and 285 in the “turnaround” region, determined from the SM abundances. Although the abundance range is narrow, just one order of magnitude, we think that there are enough galaxies in each of the three regions to obtain reliable conclusions. Finally, it has to be remarked that the abundances of all the galaxies in our sample are subsolar and any conclusion obtained in this investigation is valid only to this range of metallicity and should not be extrapolated outside it.

First, we will focus on the distribution of the abundances of the 438 galaxies of our sample.

The total abundance range is 7.6-8.5. The histogram with the SM abundances distribution is shown in Fig 2a. The peak, corresponding to the most probable value, is equal to 8.1. Thirty-two percent of the galaxies of the total sample have this abundance. One hundred and ninety-six (43%) galaxies are less metallic, and 111 (25%) are more metallic, than 8.1. Therefore, it is an asymmetric curve. The distribution determined with the  $R_{23}$  is shown in figure 2b. It is very similar to figure 2a: a large peak is at 8.1 (38% of the total sample). The main difference is the narrow range in metallicity with no galaxies more metallic than 8.3, indicating a large width of the curve. On the other hand, the distribution of the  $P$  method is very different. It shows a bimodal distribution, with two peaks corresponding to the low and high metallicity regions. Such a distribution is not observed for any other method and is likely due to the two different equations used in the determination of the abundances for high ( $>8.2$ ) and low ( $<8.2$ ) metallicity (Pilyugin & Thuan 2005). The distribution shown in figure 2c differs with the previous ones not only in the shape but also in the most common value. The low-metallicity peak is at 7.95, covering two bins in metallicity from 7.9 to 8.0. Sixty-one percent of the galaxies have  $P$  metallicities in this range. Concerning the high metallicity, the peak is at 8.3 with a total of 48% of the galaxies having such values of the abundance.

The next step is to compare the abundances from the SM and the  $R_{23}$  methods. This is shown in figure 3. The solid line is the 1:1 line, where both methods give the same abundances, while the dashed line is the dispersion of the  $R_{23}$  calibrator determined by us and without the typical uncertainty for this method. The lines are not parallel because of the differences in the dispersion in the three metallicity regions. Due to the small metallicity range, the three abundance branches are shown in one single plot, with dashed vertical lines dividing them. As seen in figure 2b, one effect of the  $R_{23}$  calibrator is to narrow the metallicity range. This can be seen also in figure 3, where only one low-metallicity galaxy has a  $R_{23}$  value lower than the SM ones. Moreover, only one high-metallicity galaxy has a  $R_{23}$  abundance higher than the SM one. In contrast, 25 (13) have higher(lower) metallicity than the value determined with the SM for low- and high-metallicity regions, when considering the uncertainties of the SM data. In order to get the goodness of the  $R_{23}$  method, the dispersion can be evaluated. It gets values of 0.15, 0.19, and 0.09 for the high, low, and “turnaround” regions (See Table 2). Finally, the percentage of data points which do not fit the  $1:1 \pm \text{dispersion}$  line are 20%, 25%, and 9% for the high, low, and “turnaround” region, respectively. Then, the values of the  $R_{23}$  method at the “turnaround” region are confident enough, in contrast to what Melbourne et al. (2004) claimed.

Figure 4 shows the same plot but for the  $P$  method. The abundances have been determined with the low-metallicity equation (Pilyugin 2000) for the galaxies in the turnaround and the low-metallicity regions and the new calibration by Pilyugin & Thuan (2005) is used for the high-metallicity region. The first thing to notice is that the distribution is not smooth now, in the sense that there is a discontinuity at 8.2. Moreover, most of the data points in the “turnaround” region do not fit the  $1:1 \pm \text{dispersion}$  line, but they give smaller metallicities than the SM ones. This might be likely because the abundance determination in the “turnaround” region was done using the low-metallicity equation, following Pilyugin (2001). But previously, he used this same equation only

for galaxies with abundances smaller than 7.95. Therefore, we can conclude that the equation for the low-metallicity branch is not entrusted for the “turnaround” region. This also can be checked using the dispersions. The value for the “turnaround” region is the highest one (0.14, compared with 0.09 and 0.11 for the high- and low-metallicity regions, respectively) but still there are 82% of the data points in this region which do not fit the  $1:1 \pm \text{dispersion}$  line.

In Table 2 we have summarized the dispersion and the fitting percentages for the two calibrations for each one of the metallicity regions. The first thing to notice is that the dispersion is not constant with metallicity for any of the semiempirical methods studied here. There is a dependence on the metallicity so a single value cannot be used for the whole range. The best numbers for the low and high regions are given by the  $P$  method, but for the “turnaround” region the best numbers are those obtained by the  $R_{23}$  method, due to the problems of the  $P$  method mentioned above. Another reason might be because the  $R_{23}$  abundances are clustered around 8.0, as can be seen in figure 2a.

With these values it can be concluded that the semiempirical methods provide values for the metallicity closer to those of the SM ( $\sigma < 0.1$ ) for six out of ten galaxies studied here. Moreover, the  $P$  method gives the closest values to the SM abundances for those data points with abundances smaller than 7.9 and larger than 8.2.

### 3.1. On the dependence of the dispersion

One of the most interesting features found in this investigation is the fact that the dispersion varies with the metallicity. In order to understand it, we study some parameters to see on which of them the dispersion depends.

In figure 5, the residuals between the SM abundance and the  $R_{23}$ (a) and the  $P$ (b) abundances are shown. The uncertainties of the SM method are shown as dotted lines. The first thing to notice is the discontinuity in the residuals for metallicities larger than 8.2 for the  $P$  method. This is probably a consequence of the two different equations used in the determination of the abundances with this method. Secondly, there is a correlation between the metallicity and the residuals, it being positive for values larger than 8.0 and negative for values lower than 8.0. Such correlation is present for both methods, the strongest being that for the  $R_{23}$  with residuals of up to 0.6, while the largest residuals for the  $P$  method is 0.43. In spite of the relationship, only 13% and 12% of the galaxies have residuals larger than 0.2 for the  $R_{23}$  and the  $P$  methods, respectively. This might indicate the low sensitivity of the semiempirical methods to the real value of the metallicity, giving values of  $8.0 \pm 0.2$  for most of the data.

Our figure 5 can be compared with Figures 5 and 6 in Pérez-Montero & Díaz (2005). They used a different metallicity range than that considered in the present investigation. Therefore, the comparison is restricted to the common metallicity range. The only difference is that they considered the differences between the semiempirical methods and the SM method. Therefore,

they got negative residuals at larger metallicities. They do not obtain any gap for values larger than 8.2 for the  $P$  method, but they present the low and high metallicity branches in two different figures and so the gap might be difficult to see. Their residuals are larger than our values but the correlation is similar. They also found out that the larger values of the residuals are for abundances of around 7.6, diminishing for lower metallicities. As we do not have in our sample very low metallicity galaxies ( $12+\log(\text{O}/\text{H}) < 7.6$ ) we cannot investigate this point with our more homogeneous sample.

We can study whether there is any other dependence on the residuals. In particular we are interested in the possible relation between the residuals and the ionization parameter,  $([\text{O II}]/[\text{O III}])$ , mainly because both methods used here claim that such a parameter is considered in the calibrations. The relationship between the  $([\text{O II}]/[\text{O III}])$  ratio and the residuals of the  $R_{23}$  is shown in figure 6a, while figure 6b shows the same relationship for the  $P$  abundance. The behaviour for both, the  $R_{23}$  and the  $P$  residuals with the  $([\text{O II}]/[\text{O III}])$  ratio are very similar: for those galaxies with  $\log([\text{O II}]/[\text{O III}]) > 1.0$  (high-ionization regions) the residuals get more negative, indicating that the abundances determined with the semiempirical methods are larger than the SM ones.

Another interesting parameter will be the equivalent width of  $\text{H}\beta$ ,  $\text{EW}(\text{H}\beta)$ . This is a good age indicator (see section 3.2). The plot between the residuals and the  $\text{EW}(\text{H}\beta)$  is shown in figure 7. In this case, there is no clear trend, apart from the fact that for those galaxies with  $\text{EW}(\text{H}\beta)$  smaller than 30 and larger than 150, the residuals are more negative for the  $R_{23}$  method. The trend is similar for the  $P$  method but the dispersion is larger.

In conclusion, it can be said that the residuals depend mainly on the abundances and, probably on the ionization parameter.

### 3.2. The influence of the age of the regions

Pérez-Montero & Díaz (2005) from their study of the semiempirical methods concluded that there are not many ways to improve the  $R_{23}$  and the  $P$  methods because of their dependence on the ionization parameters and ionization temperatures. These parameters change as the H II evolve in a way that is not easy to parametrize.

In order to check the influence of the difference of the age of the star formation bursts we can divide the sample considering their morphological types. It is well known that blue compact galaxies (BCG) are experiencing right now an intense burst of star formation, while the events of star formation in both late spirals (Sm) and irregular (Im) galaxies are less intense. In consequence, the ionization parameter and temperatures might be different for these three subsamples of galaxies, and therefore, the  $R_{23}$  and  $P$  abundances. The main caveat is that the differences between these morphological types are very subtle, especially between the BCG and the Im. It is considered that BCG have younger bursts of star formation, but their  $\text{EW}(\text{H}\beta)$  range is between 14 and 280, according to table 2 in Kniazev et al. (2004). Such values might indicate that the ages of the

present burst in the BCG are between 4 and 10 Myr for a Salpeter IMF and an upper limit mass of  $120 M_{\odot}$ , following the Copetti et al. (1986) models. Moreover, all the Sm and 18 of the Im have  $EW(H\beta)$  smaller than 50. Therefore, it can be concluded that not all the BCG have truly young H II regions but some of them are as old as the bursts in Sm and Im. In contrast, all the Sm have old bursts. In consequence, the morphological type is not a good approach to study the influence of the age.

Another approach to the problem of the age/evolution of the regions is using a parameter to discriminate between truly “old” and “young” H II regions. As previously said, equivalent width of  $H\beta$  has been considered as a good age indicator (Copetti et al. 1986). Therefore, we can explore such parameter in our sample in order to see the age effect. The first thing to notice is that 269 out of the 438 galaxies have values of the  $EW(H\beta)$  smaller than 50, independently of the morphological type. This  $EW(H\beta)$  implies an age of the burst of at least 8 Myr, and it is quite independent of the parameters of the models (Copetti et al. 1986). Another interesting fact is that only 19 galaxies with  $EW(H\beta)$  larger than 50 have low abundances, while 69 of the galaxies with  $EW(H\beta)$  smaller than 50 show a low metal content.

Finally, we can explore the goodness of the  $R_{23}$  and the  $P$  method using this parameter. Figure 8 shows the SM versus  $R_{23}$  (Figure 8a) and the SM versus  $P$  (Figure 8b) abundances, but now the galaxies with  $EW(H\beta)$  larger than 50 are plotted as triangles. It is interesting to see that the majority of the galaxies which do not fit the  $1:1 \pm \text{dispersion}$  line have  $EW(H\beta) > 50$  (53 out of 70) with the  $R_{23}$ . The plot of the  $P$  method is more complex: at low metallicity all of the galaxies outside the  $1:1 \pm \text{dispersion}$  line have  $EW(H\beta) > 50$ , while at the “turnaround” region it is the opposite. At high metallicity, only half of the sample outside the  $1:1 \pm \text{dispersion}$  line have large values of the  $EW(H\beta)$ . The conclusion emerging from these plots is that those galaxies with younger bursts of star formation might have large discrepancies between the SM and the  $R_{23}$  (or  $P$ ) abundances.

#### 4. Comparison with other investigations

The comparison of the different semiempirical methods against the SM has been done before (e.g., Pérez-Montero & Díaz 2005 and references therein). All of them follow the same procedure. In order to create a large sample the authors gathered data from the literature. These data were very heterogeneous in many ways: they were observed with different apertures, were analyzed by different persons with different criteria (see A.M. Hidalgo-Gómez 2009, in preparation, for a study of the variation in the SM abundances due to these effects), etc. Therefore, the results cannot be completely reliable. The dispersion might account for the differences in the acquisition/reduction/analysis procedure. In this sense, the sample studied here is completely homogeneous. It is large enough to obtain conclusive results. Another advantage of the results presented in Section 3 is that the range in metallicity has been divided into the three typical branches and therefore they can be studied in more detail. Here we are going to compare our results with

some of the most recent investigations. The only caveat is that the results are restricted to the abundance range studied here and should not be extrapolated outside it.

Lee et al. (2003) made a comparison between the SM and the  $R_{23}$  calibrator concluding that most of the data was consistent with the  $1:1 \pm 0.2$  dex line. These uncertainties are too relaxed, as can be seen in Table 2. But when the uncertainty is only 0.1, more than half of their data are located outside the region, consistent with the result presented here. Moreover, they did not make the separation into the three branches. When such a division is done, 38%, 70%, and 50% of the galaxies do not lay in the  $1:1 \pm 0.1$  dex. These values are again very similar to those presented here.

Kennicutt et al. (2003) made a comparison between the SM abundance and the  $R_{23}$  one for H II regions with metallicities larger than 8.0. Their sample is much smaller than the one presented here. Their  $R_{23}$  metallicities are higher than their SM abundances. This is the opposite of what we found here. Several reasons might play a role: the differences in aperture among the galaxies in their sample, the morphological differences, or a problem with the photoionization models used in the  $R_{23}$  calibration from Kewley & Dopita (2002), as they discuss. Surprisingly, the dispersions are very similar to those in figure 3. They also compared the  $P$  metallicity (old calibration) with the SM abundances. For high metallicity, their  $P$  value is higher than or equal to the SM value, but at metallicity  $\approx 8.0$  the  $P$  abundance is lower than the SM abundance. Although we did not study the old calibration of the  $P$  method, a similar trend is found in Figure 4, using the new calibration. Also, the dispersion at high metallicity is similar in both investigations in spite of the differences in the sample size.

Pérez-Montero & Díaz (2005) conducted a study of the different nebular calibrator and photoionization models. They used several calibrations for the  $R_{23}$  abundance but we focus on their results with the McGaugh (1991) calibration because this is the calibration used in the present investigation. They used a heterogeneous sample with data from different sources in the literature. They found that at high abundance the  $R_{23}$  abundances are larger than those with the SM with a dispersion of  $\approx 0.7$ . For low metallicities, the results are similar to those shown in figure 3, but with larger dispersion. They also compared the  $P$  abundances; again, they found similar results to those found in the present investigation, but with larger dispersion.

Recently, Shi et al. (2006) presented a comparison between the SM and several semiempirical methods similar to the one presented here. Their main advantage is the number of data points: a total of 4222. But their main drawback is that they did not use the SM method for 3997 galaxies, where the [O III]  $\lambda 4363$  line was not detected. Instead, they used equation 11 in Pilyugin (2001) to determine the  $T_e$  and afterwards, the relations by Garnett (1992) and Pagel et al. (1992) to determine the rest of the parameters. Therefore, their sample is not self-consistent because they mixed different methods in the determination of the oxygen abundances of a single galaxy. So, the oxygen abundances of their sample II cannot be used for comparing the different methods. The main advantage is that their sample is not biased to galaxies with the oxygen line [O III]  $\lambda 4363$ . In any case, and considering only their sample I of 225 galaxies, their results are very similar to those

presented here for the  $R_{23}$  and the  $P$  calibrator.

Finally, Liang et al. (2006) studied the different calibrators with a very large sample (over 40,000 galaxies). Again, they have to use the  $R_{23}$  calibrator in order to determine the abundances for most of the galaxies of their sample. The small metallicity range in common between their sample and the study presented here makes any comparison meaningless.

## 5. Discussion

Melbourne et al. (2004) made a comparison of the abundances determined with the SM and the  $P$  calibrator. They found that the most deviating galaxies of their sample of low-metallicity galaxies correspond to those with the lower excitation indicator ( $[\text{OIII}]/[\text{OII}]$ , as defined by them) and high electronic temperature. Figures 9 and 6 show the  $T_e$  and the  $[\text{OII}]/[\text{OIII}]$  versus the residuals between the SM and the  $P$  methods, respectively. For low-metallicity galaxies we obtained the same results as Melbourne et al. (2004): the most deviating galaxies, defined as those with  $SM - P > 0.2$ , are those with  $T_e$  larger than 14,000 K. In the case of those galaxies with high metallicity the most deviating are those with  $T_e$  smaller than 10,000 K (11,000 K in the  $P$  method). The most deviating galaxies in the “turnaround” region have low  $T_e$ , just the opposite of that in the low-metallicity region. This behaviour might be due to the correlation shown in figure 1 for galaxies with  $T_e$  larger than 14,000 K, because larger abundances mean lower  $T_e$  and lower  $[\text{OII}]/[\text{OIII}]$ , but it is not related to any physical properties of the galaxies.

In any metallicity range the cutoff in the ionization parameter is not that clear. The only trend is that those galaxies with a low ionization parameter have a semiempirical oxygen abundances that are similar to the SM value ( $\pm 0.2$ ). The discrepancy with the SM abundances is larger for those galaxies with larger values of the ionization parameter.

## 6. Conclusions

We have made a detailed comparison of the abundances obtained with the so-called standard method (SM) and some of the semiempirical methods used:  $R_{23}$  (McGaugh’s calibration) and  $P$  (Pilyugin & Thuan 2005). Our main interest is to obtain the closest abundances to the SM abundances when the standard method cannot be applied. In order to do that we used a large sample of late-type galaxies observed by SDSS and reduced by Kniazev et al. (2004). For all of the galaxies in the sample the oxygen forbidden line  $[\text{O III}]\lambda 4363$  is detected, and therefore the SM abundances can be determined. The main advantage of this sample is that it is large enough for obtaining conclusive results and very homogeneous (being observed by only one facility and reduced and analyzed in the same way for all the galaxies); therefore, the systematic errors will affect all the data in the same way. This is not the usual procedure in the literature, where data, gathered from different sources, are obtained from different facilities, and analyzed and reduced by

different researchers. A.M. Hidalgo-Gómez (2009, in preparation) found that this procedure might be a large source of uncertainties in the abundances determination. One of the disadvantages of the sample is that the use of only those galaxies where the auroral oxygen line was detected restricts the metallicity range, especially at high metallicity. Therefore, and keeping this last statement in mind, the conclusions obtained in this investigation are restricted to sample with similar metallicity range and characteristics.

The main conclusions could be listed as follows.

1- The distribution of the metallicity of the galaxies is a single gaussian for both the SM and the  $R_{23}$  method. The main differences between them is the smaller width of the gaussian for the  $R_{23}$  abundances. This clustering of the  $R_{23}$  abundances around a single value ( $\approx 8.05$ ) is clearly visible at figures 2b and 3. Such behaviour might be real or due to the sample itself, which is restricted to an “special” type of galaxies (those with the auroral oxygen line detected). Moreover, as the number of this type of galaxies is a tiny fraction of the total SDSS catalog, SDSS imposes important bias to any sample. In order to find out if the clustering is real, a similar study has to be done with other large sample obtained from choosing the galaxies observed without any “a priori” assumption.

2- The  $P$  calibration gives the lowest dispersion in both the high- and the low-metallicity regions, while the  $R_{23}$  gives the best results in the “turnaround” region.

3- For both methods, there is a dependence of the dispersion with the metallicity for the low- and high-metallicity regions, while they are very insensitive to the metallicity in the “turnaround” region.

4- There is a dependence of the residuals with the abundances and the  $T_e$  for both methods. For galaxies with  $\log[\text{O II}]/\text{O III}] > 1$ , the residuals are larger.

5- Finally, those galaxies with larger values of the equivalent width of  $\text{H}\beta$  seem to have very different abundances than the SM abundances, especially at low metallicity, but there is no clear trend between the residuals and the  $\text{EW}(\text{H}\beta)$ .

Finally, we might note that the results obtained here are similar to those found in other investigations, but due to the large and homogeneous sample used here, the results are more robust and the dispersion lower than in previous investigations.

The authors thank J. González and C. Morisset for many interesting suggestions which improved the paper and to J. Brenan for a carefully reading of the manuscript. The referee, Angeles Díaz, is thanked for many interesting comments which have improved the manuscript. A.M.H-G. thanks J.M. Vílchez for very interesting discussions. This investigation was supported by DGAPA-UNAM grant IN114107 and CONACyT CB-2006.

## REFERENCES

- Aller, L.H. 1984, “Physics of Thermal Gaseous Nebulae”, (Dordrecht: Reidel)
- Campbell, A., Terlevich, R., & Melnick, J. 1986, MNRAS, 223, 811
- Copetti, M.V.F., Pastoriza, M.G., & Dottori, H.A. 1986, A&A, 156, 111
- Deharveng, L., Peña, M., Caplan, J., & Costero, R. 2000, MNRAS, 311, 329
- Denicoló, G., Terlevich, R., & Terlevich, E. 2002, MNRAS, 330, 69
- Díaz, A.I. & Pérez-Montero, E. 2000, MNRAS, 312, 130
- Garnett, D.R. 1992, AJ, 103, 1330
- Hägele, G.F., Díaz, A.I., Terlevich, E., Terlevich, R., et al. 2008, MNRAS, 383, 209
- Hoyos, C., & Díaz, A.I. 2006, MNRAS, 365, 454
- Izotov, Y.I., Stasińska, G., Meynet, G., Guseva, N.G., & Thuan, T.X. 2006, A&A, 448, 955
- Kennicutt, R.C.Jr., Bresolin, F. & Garnett, D.R. 2003, ApJ, 591, 801
- Kewley, L.J., & Dopita, M.A. 2002, ApJS, 142, 35
- Kewley, L.J. & Ellison, S.L. 2008, ApJ, 681, 1183
- Kniazev, A.Y., Pustilnik, S.A., Grebel, E.K., Lee, H. & Promskij, A.G. 2004, ApJS, 153, 429
- Kobulnicky, H.A. & Kewley, L.J. 2004, ApJ, 617, 240
- Lee, H., McCall, M.L. & Richer, M.G. 2003, AJ, 2975
- Liang, Y.C., Yin, S.Y., Hammer, F., Deng, L.C., Flores, H., & Zhang, B. 2006, ApJ, 652, 257
- Mathis, J.S. 2000, ApJ, 544, 347
- McGaugh, S.S. 1991, ApJ, 380,140
- Melbourne, J., Phillips, A., Salzer, J.J., Gronwall, C., & Sarajedini, V.L. 2004, AJ, 127, 686
- Melbourne, J., & Salzer, J.J. 2002, AJ, 123, 2302
- Olofsson, K. 1997, A&A, 321, 290
- Oey, M.S. & Shields, J.C. 2000, ApJ, 539, 687
- Osterbrock, D.E. 1989 *Astrophysics of Gaseous Nebulae and Active Galactic Nuclei*, (University Science Books, Mill Valley, CA)

- Pagel, B.E.J., Simonson, E.A., Terlevich, R.J., & Edmunds, M.G. 1992, MNRAS, 255, 325
- Pagel, B.E.J., et al. 1979, MNRAS, 189, 95
- Peimbert, M. & Torres-Peimbert, S. 1977, MNRAS, 179, 217
- Pérez-Montero, E. & Díaz, A.I. 2003, MNRAS, 346, 105
- Pérez-Montero, E. & Díaz, A.I. 2005, MNRAS, 361, 1063
- Pettini, M. & Pagel, B.E.J. 2004, MNRAS, 348, 59
- Pilyugin, L.S. 2000, A&A, 362, 325
- Pilyugin, L.S. 2001, A&A, 369, 594
- Pilyugin, L.S. & Thuan, T.X. 2005, ApJ, 631, 231
- Pilyugin, L.S., Vílchez, J.M. & Thuan, T.X. 2006, MNRAS, 370, 1928
- Shi, F., Kong, X., & Cheng, F.Z. 2006, A&A, 453, 487
- Stasińska, G. 1980, A&AS, 48, 299
- Thuan, T.X. 2008, Proceedings of the conference “Low-metallicity star formation: from first stars to dwarf galaxies” Ed: Hunter, Manden & Schneider
- Zaritsky, D., Kennicutt, R.C.Jr., & Huchra, J.P. 1994, ApJ, 420, 87

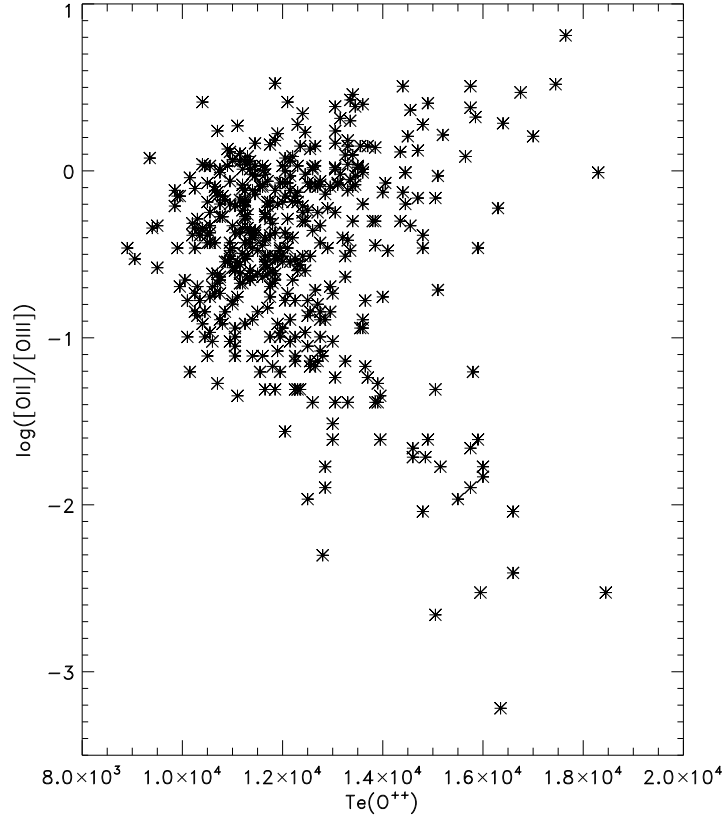


Fig. 1.— Electron temperature vs. the  $\log[\text{O II}]/[\text{O III}]$  ratio. The bulk of galaxies in the sample, with temperature lower than 14,000 K, do not show any relationship with the ionization parameter. For those galaxies with  $T_e$  higher than 14,000 K there are two different trends: some of them have low values of the  $\log[\text{O II}]/[\text{O III}]$  ratio while some others show values of this ratio about 1.

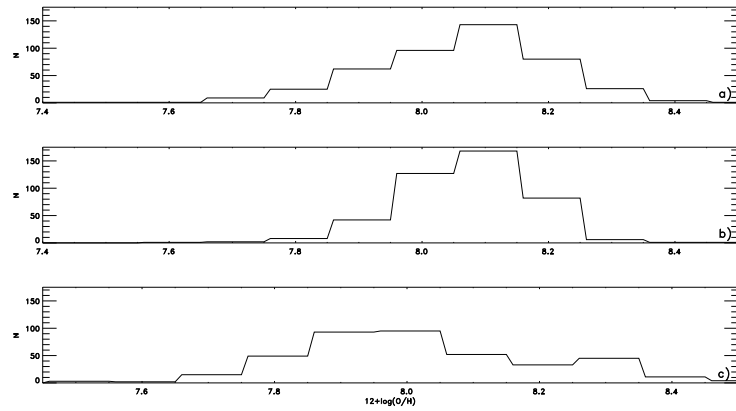


Fig. 2.— The metallicity distribution of the total of 438 galaxies studied in the present investigation. The metallicity has been determined with the standard method (a), the  $R_{23}$  method (b), and the 2005 calibration of the  $P$  method (c). The distribution of the two first methods is very similar, while the  $P$  method gives a bimodal distribution due to the two different equations used for the metallicity determination.

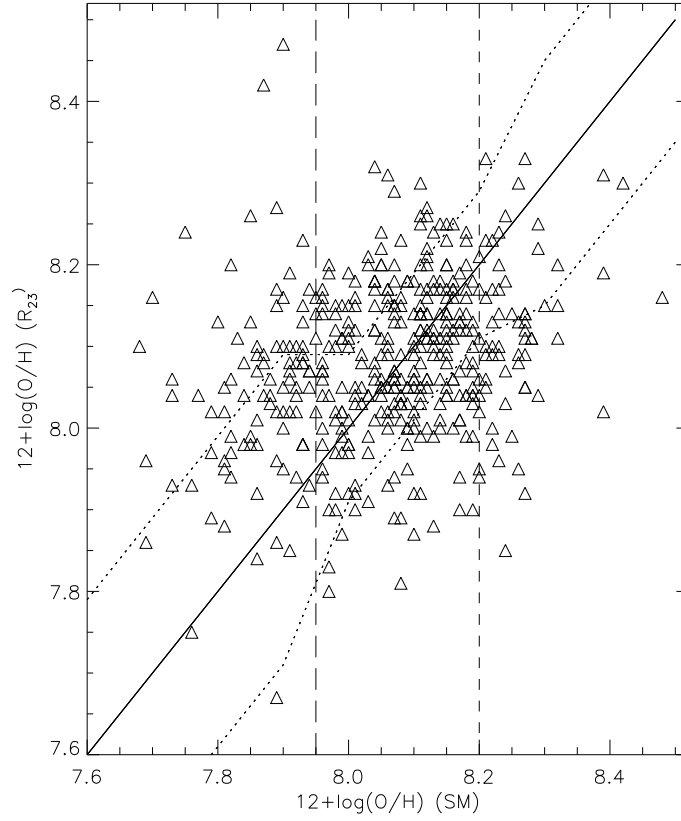


Fig. 3.— The metallicity determined with the SM method vs. the  $R_{23}$  method for the 438 galaxies in the sample. The solid line is the 1:1 line while the dashed ones are the dispersion. As the dispersion depends on the metallicity, they are not parallel.

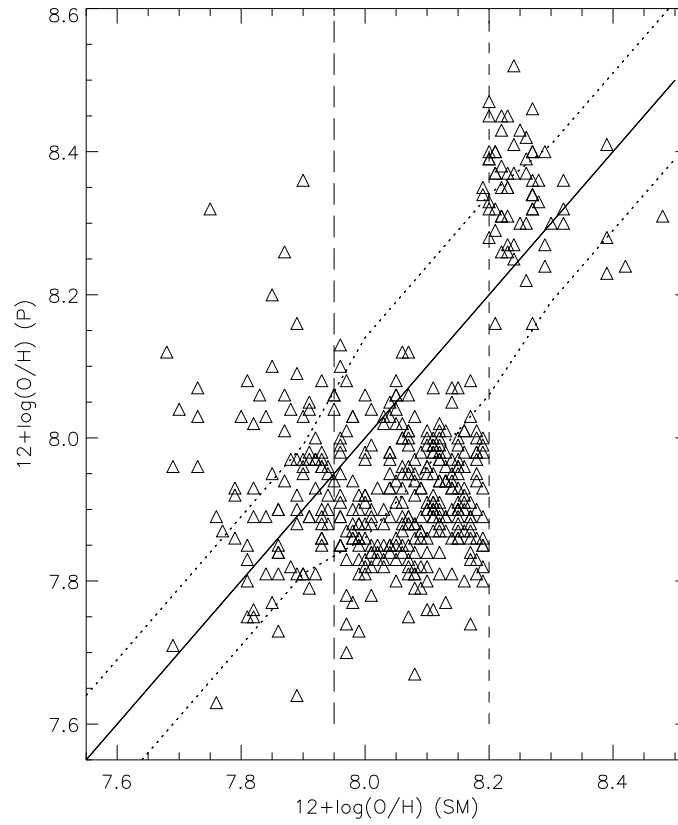


Fig. 4.— The metallicity determined with the SM method vs. the  $P$  method for the 438 galaxies in the sample. Symbols and lines as in figure 3.

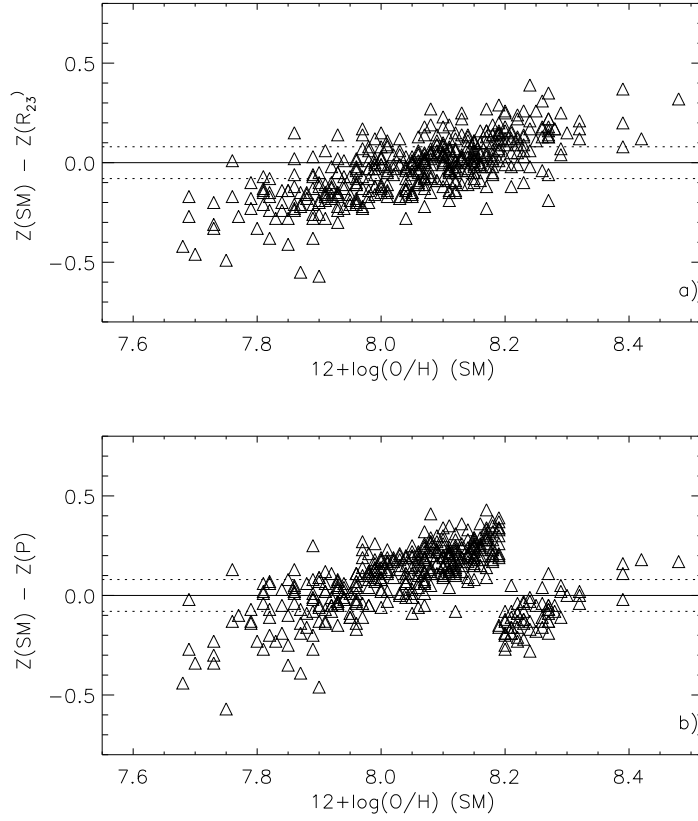


Fig. 5.— Residuals between the SM and the  $R_{23}$ (a) and the  $P$ (b) methods vs. the SM abundances for the 438 galaxies in the sample. The solid line at 0.0 indicates that both methods give the same value of the abundance, while the dashed lines are the uncertainties of the SM method.

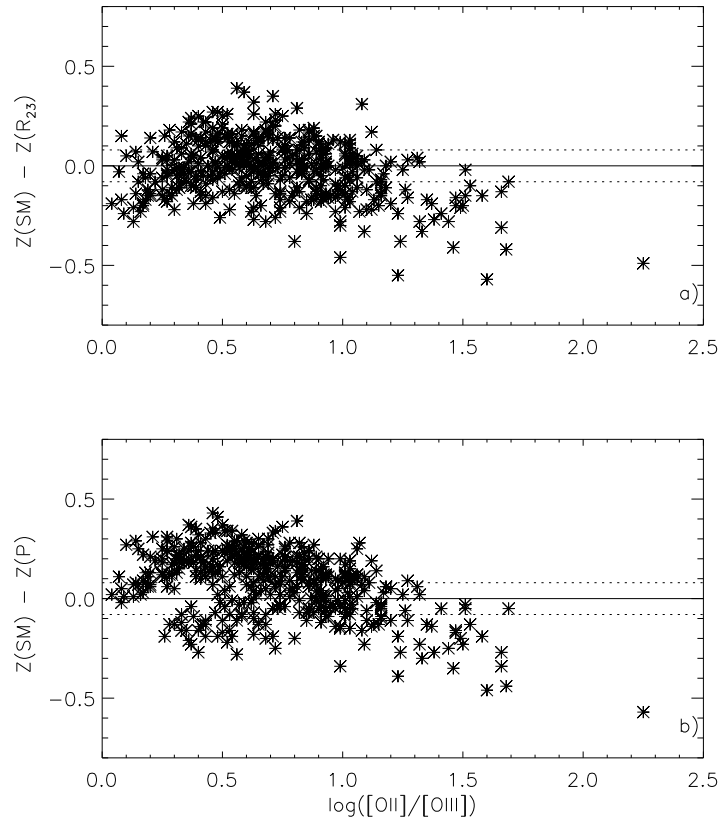


Fig. 6.— Residuals between the SM and the  $R_{23}$  (a) and the  $P$  (b) methods vs. the  $\log[\text{O II}]/[\text{O III}]$  ratio. Lines as in figure 5.

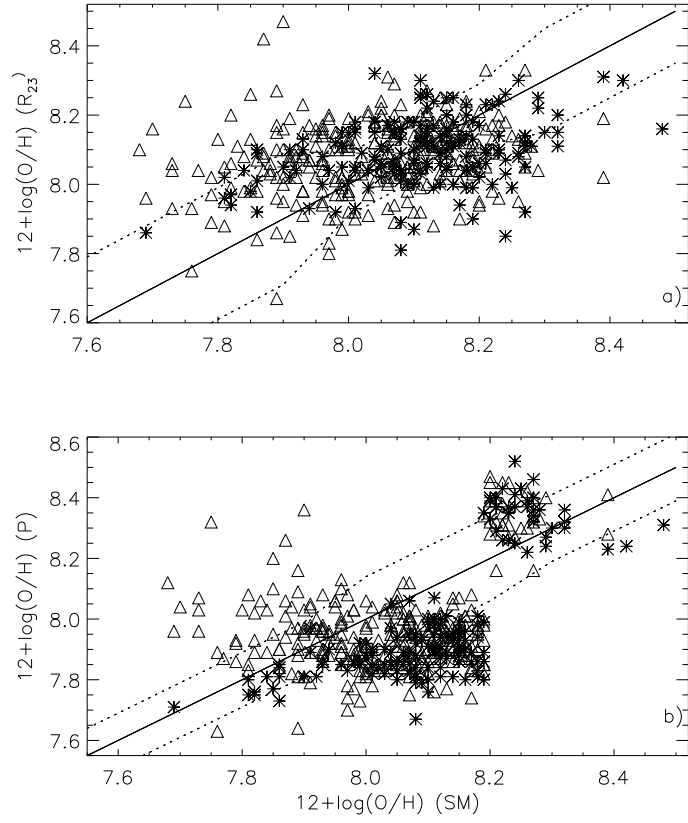


Fig. 7.— The metallicity determined with the SM method vs. the  $R_{23}$ (a) and the  $P$ (b) methods for those galaxies with  $\text{EW}(\text{H}\beta) > 50$  (triangles) and smaller than 50 (crosses). Lines as in figure 3.

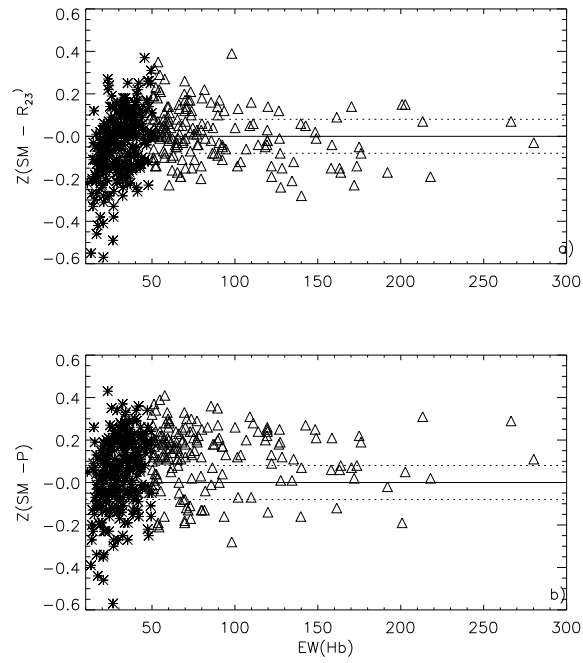


Fig. 8.— Residuals between the SM and the  $R_{23}$  (a) and the  $P$  (b) methods vs. the equivalent width of  $\text{H}\beta$ . Triangles represent those galaxies with  $\text{EW}(\text{H}\beta)$  larger than 50 and crosses those galaxies with  $\text{EW}(\text{H}\beta)$  smaller than 50. Lines as in figure 6.

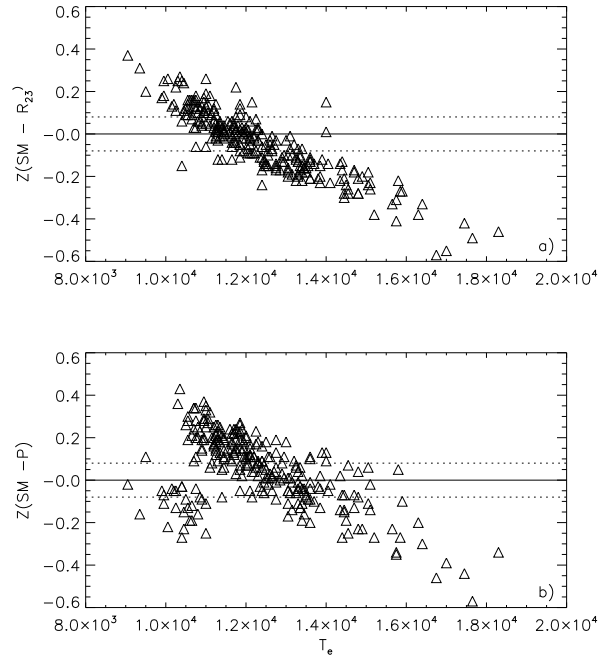


Fig. 9.— Residuals between the SM and the  $R_{23}$  (a) and the  $P$  (b) methods vs. the electron temperature. Half of the galaxies with  $T_e$  larger than 14,000 K present a deviation larger than 0.2. Lines as in figure 6.

Table 1: Differences Between the Oxygen Abundance Values determined with the code used in the present investigation and those of Kniazev et al. (2004) (column 1), Izotov et al. (2006) (column 2) and Aller (1984) (column 3). The second row shows the percentage of abundances values with differences smaller than the SM uncertainties while the percentage of identical abundance values are shown in row 3.

$\Delta Z_K$	$\Delta Z_I$	$\Delta Z_A$
0.012	0.15	0.02
3.4%	70%	5%
27%	0%	20%

Table 2: Dispersion (top line) and fitting percentages (bottom line) for each of the metallicity regions given by the semiempirical methods studied here. The first column lists the regions, while the dispersion and percentages of the  $R_{23}$  and  $P_n$  are given in columns 2, 3 and 4.

Metallicity	$R_{23}$	$P_n$
high	0.15	0.09
	59%	55%
turnaround	0.09	0.14
	64%	62%
low	0.19	0.11
	62%	68%